

Development of a micro-thrust measurement system and ground thrust measurement of the micro Hall thruster for Taiji mission

Shengtao Liang^{a,b,c,*}, Luxiang Xu^{a,c,**}, Shixu Lu^{a,b}, Liexiao Dong^{a,b},
Mingshan Wu^{a,c}, Jianfei Long^{a,c}

^a School of Fundamental Physics and Mathematical Sciences, Hangzhou Institute for Advanced Study, UCAS, Hangzhou, 310024, China

^b University of Chinese Academy of Sciences, 100049, Beijing, China

^c Taiji Laboratory for Gravitational Wave Universe, Hangzhou Institute for Advanced Study, UCAS, Hangzhou, 310024, China

ARTICLE INFO

Keywords:

Electric propulsion
Hall thruster
Taiji mission

ABSTRACT

The Taiji Laboratory for Gravitational Wave Universe has developed a micro-thrust measurement system specifically for ground thrust measurement of a micro Hall thruster. The thrust measurement system's core component is the thrust stand, which is designed based on a hanging pendulum topology and has undergone four generations of iterative optimization. This thrust measurement system is capable of measuring the thrust in the range of 0–100 μN with a resolution better than 0.1 μN . This study presents ground thrust measurements for a ground-optimized version of the micro Hall thruster on board the Taiji-1 satellite. The Taiji-1 micro Hall thruster is currently the lowest power level Hall thruster in orbit and has a unique physical design that allows it to operate without an external cathode. The thrust measurement results demonstrate that the ground-optimized thruster can provide continuous thrust modulation in the range of 0.94–104.67 μN , with a resolution superior to 0.2 μN . This research provides technical support for ground testing and iterative optimization of micro-thrusters for the Taiji gravitational wave detection mission.

1. Introduction

Gravitational waves are a very significant prediction of Einstein's general theory of relativity [1]. Since 2015, gravitational waves have been proven to exist, marking a new era in detecting gravitational waves [2]. Space-based gravitational wave detection covers a wider range of gravitational wave signal sources and provides a deeper and broader understanding of the universe compared to ground-based gravitational wave detection [3]. Therefore, international research primarily focuses on the detection of gravitational waves in space. This involves using satellite formations to detect gravitational wave signals by building large laser interferometers in space. The LISA mission has been proposed by the European Space Agency, while Japan has proposed the DECIGO future space gravitational wave antenna [4,5]. In China, the Taiji and Tianqin missions have been proposed for conducting gravitational wave detection [6].

The micro-thruster is a vital component for the space gravitational wave detection project, which generates micro-thrust in real time to

counteract non-conservative forces, such as solar radiation light pressure, to keep the satellite in a drag-free control state [7,8]. Compared to traditional chemical propulsion, electric propulsion offers faster thrust response and more precise thrust adjustment, making it highly suitable for gravitational wave detection missions [9,10]. Several research institutions have conducted studies on micro electric thrusters and have achieved significant advancements. Currently, electric thrusters that have advantages in the field of gravitational wave detection include the micro Hall thruster, the radio frequency ion thruster, the microwave ion thruster, and the cusped field thruster [11–16]. Compared to other thrusters, micro Hall thrusters can discharge without external neutralizers, radio frequency, and microwave sources, which have the advantages of a simple structure, light weight, compact size, and fast response. Notably, on August 31, 2019, the Taiji-1 satellite, China's first essential technology verification satellite for gravitational wave detection, was launched into space using micro Hall thrusters as its engine [17,18]. The micro Hall thruster used for the Taiji-1 satellite was jointly developed and researched by Nanyang Technological University and our team

* Corresponding author. School of Fundamental Physics and Mathematical Sciences, Hangzhou Institute for Advanced Study, UCAS, Hangzhou, 310024, China.

** Corresponding author. School of Fundamental Physics and Mathematical Sciences, Hangzhou Institute for Advanced Study, UCAS, Hangzhou, 310024, China.

E-mail addresses: liangshengtao1994@163.com (S. Liang), xuluxiang@ucas.ac.cn (L. Xu).

<https://doi.org/10.1016/j.actaastro.2025.01.047>

Received 26 March 2024; Received in revised form 5 January 2025; Accepted 20 January 2025

Available online 23 January 2025

0094-5765/© 2025 The Authors. Published by Elsevier Ltd on behalf of IAA. This is an open access article under the CC BY-NC license (<http://creativecommons.org/licenses/by-nc/4.0/>).

[19]. The Taiji-1 micro Hall thruster is currently the Hall thruster with the lowest power level in orbit. The micro Hall thruster is a scaled-down design of the traditional Hall thruster; however, it exhibits significant differences from the traditional thruster. The discharge voltage of a traditional Hall thruster is typically less than 600 V, whereas the operating voltage of a micro Hall thruster can reach 2000 V, with a discharge current of less than 10 mA. A distinguishing feature of traditional Hall thrusters is the reliance on a cathode as an electron source, which serves to ionize the neutral gas and thereby produce ions. The subsequent ejection of these ions from the channel generates thrust. The micro Hall thruster examined in this study exhibits a unique physical configuration that eliminates the requirement for an external cathode. This breakthrough offers potential advantages in detecting gravitational waves in space, particularly from a systems and reliability engineering perspective. The on-orbit test results demonstrate that the Taiji-1 micro Hall thruster can provide a thrust dynamic range of 5–50 μN . However, the micro Hall thruster has some disadvantages, including large plume divergence and poor thrust resolution. As a result, research on optimizing the structure of the micro Hall thruster has been ongoing since 2019.

During the iterative optimization process of the micro Hall thruster in a ground environment, it is necessary to use a vacuum chamber to simulate the space environment and conduct discharge characteristic tests on the thrusters in order to obtain key performance parameters, such as thrust, efficiency, and specific impulse [20,21]. Accurate measurement of thrust is particularly important as it is one of the most crucial parameters. Through the ground thrust test system, we can obtain the thrust performance of the developed thruster and identify the impact of different structural parameters on its thrust characteristics [22]. This provides valuable guidance during the design and optimization process of micro thrusters, which can help reduce the iteration cycle and development costs. Therefore, the micro-thrust measurement system plays an important role in the optimization and development process of micro Hall thrusters. For micro Hall thrusters, it is difficult to measure thrust using traditional methods such as force sensors or electronic balances. In the field of electric propulsion, the typical method of thrust measurement is to mount the thruster on a thrust stand and convert the difficult-to-measure thrust value into other physical quantities that are easier to measure, such as displacement [23]. This allows for the determination of the thrust value through displacement measurement. Currently, the development of milli-Newton level thrust stands is relatively mature, and many institutions have developed various thrust stands to meet different thrust measurement requirements [24,25]. However, the research on micro-Newton thrust stand devices is insufficient, and the related technology development is not yet mature. According to current research, micro-Newton thrust stands are divided into two main categories: torsion pendulum and hanging pendulum [26–29].

The torsion pendulum device is advantageous for micro-thrust measurement due to its high sensitivity [30]. However, it has a relatively weak load capacity. The Taiji mission requires a ground thrust stand with an 8 kg load capacity, which is difficult to achieve using torsion pendulum technology. In contrast, the hanging pendulum has a superior load capacity. The hanging pendulum developed by Polzin can support a total weight of 125 kg, utilizing gravity as a restoring force and providing high stability [31]. The sensitivity of the thrust measurement system can be improved by increasing the length of the rotating arm. Despite the extensive utilization of hanging pendulum technology in the field of thrust measurement of milli-Newton level Hall thrusters, there is a paucity of research on the use of hanging pendulums for ground thrust testing of micro-Newton Hall thrusters. The extremely low micro-Newton thrust generated by micro Hall thrusters imposes more stringent requirements on the stability and calibration accuracy of the ground test system. In light of these challenges, the present study aims to develop a high-load and high-resolution micro-Newton thrust measurement system. The study employs a continuous and iterative

optimization of the hanging pendulum topology, with the objective of establishing technical reserves for the subsequent advancement of micro Hall thrusters. The Taiji Gravitational Wave Universe Laboratory has developed four generations of ground thrust measurement hanging pendulums specifically for micro Hall thrusters in recent years. Based on the latest version of the thrust measurement system, the ground thrust measurement of the micro Hall thruster is investigated and reported for the first time in this paper.

2. Experimental setup

2.1. Thrust measurement system

The experiment was conducted at the Taiji Laboratory for Gravitational Wave Universe, located at the Hangzhou Institute for Advanced Study. Fig. 1 shows the experimental system utilized to measure the thrust of the micro Hall thruster. The system comprises a vacuum chamber, a thrust stand, a capacitive displacement sensor, a power supply system, a displacement acquisition system, and a data processing system.

During the thruster discharge process, the vacuum chamber, which has a diameter of 1.2 m, is maintained at a pressure of less than 3×10^{-3} Pa. The thruster anode is powered by a Keithley 2290E-5 power supply. The anode wire and propellant pipe, which have relatively small diameters, are suspended vertically from the top of the vacuum chamber to minimize their impact on thrust measurement [32]. The capacitance sensor and displacement acquisition system used is the CSH05-CAM1.4. The data acquisition system is built using LabVIEW. The discharge current, the discharge voltage of the thruster, and the displacement value of the thrust stand rotating arm were recorded through the data processing system. A camera captured the discharge plume of the thruster through the glass of the vacuum chamber. The thrust stand was designed based on the hanging pendulum topology, which utilizes gravity as the main restoring force and has advantages in terms of simplicity and stability. The hanging pendulum structure provides sufficient sensitivity for micro-thrust measurements, making it an ideal choice for this study. The thrust stand consists of a spring, a rotating arm, and a thruster mounting plate. During the experiment, both the thruster and the thrust stand were placed inside the vacuum chamber. The thruster generated a steady-state force, causing the spring to bend by an angle of θ . Simultaneously, the rotating arm produced a displacement of d , which was measured by the capacitive displacement sensor to determine the thrust value.

2.2. Thrust stand

During the initial stages, three generations of hanging pendulum thrust stands were developed to verify various technical solutions, as depicted in Fig. 2. The first two generations of thrust stands were developed jointly by our team and Southeast University [33,34]. The first generation is a thrust stand made of carbon fiber for principle verification, with a rotating arm length of 1.8 m. The experiment was conducted in a 3 m vacuum chamber due to the stand's large size. The spring utilizes an elliptical notch flexible hinge structure to achieve a high load capacity. Counterweights of varying masses were gradually added to the top of the thrust stand to test its load capacity. The results indicate that the thrust stand can withstand a maximum load of 6 kg. To generate the standard force, an electrostatic comb made up of aluminum comb teeth and Teflon insulators was placed at the bottom of the thrust stand. The first-generation thrust stand's rotating arm length was chosen to be 1.8 m to improve system sensitivity and obtain better thrust resolution. However, this excessive arm length resulted in increased machining and assembly errors, as well as exacerbated the problem of thermal drift caused by temperature changes. As a result, a smaller second-generation version of the thrust stand was developed, with a 0.2 m rotating arm made of quartz. Based on the second-generation thrust

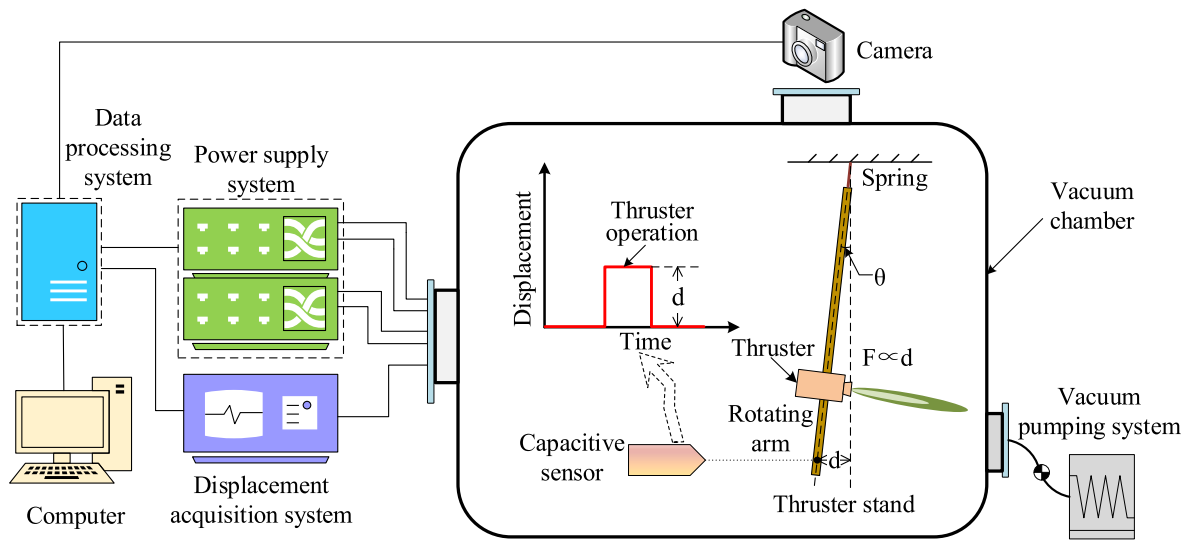


Fig. 1. Experimental system setup for micro Hall thruster thrust measurement.

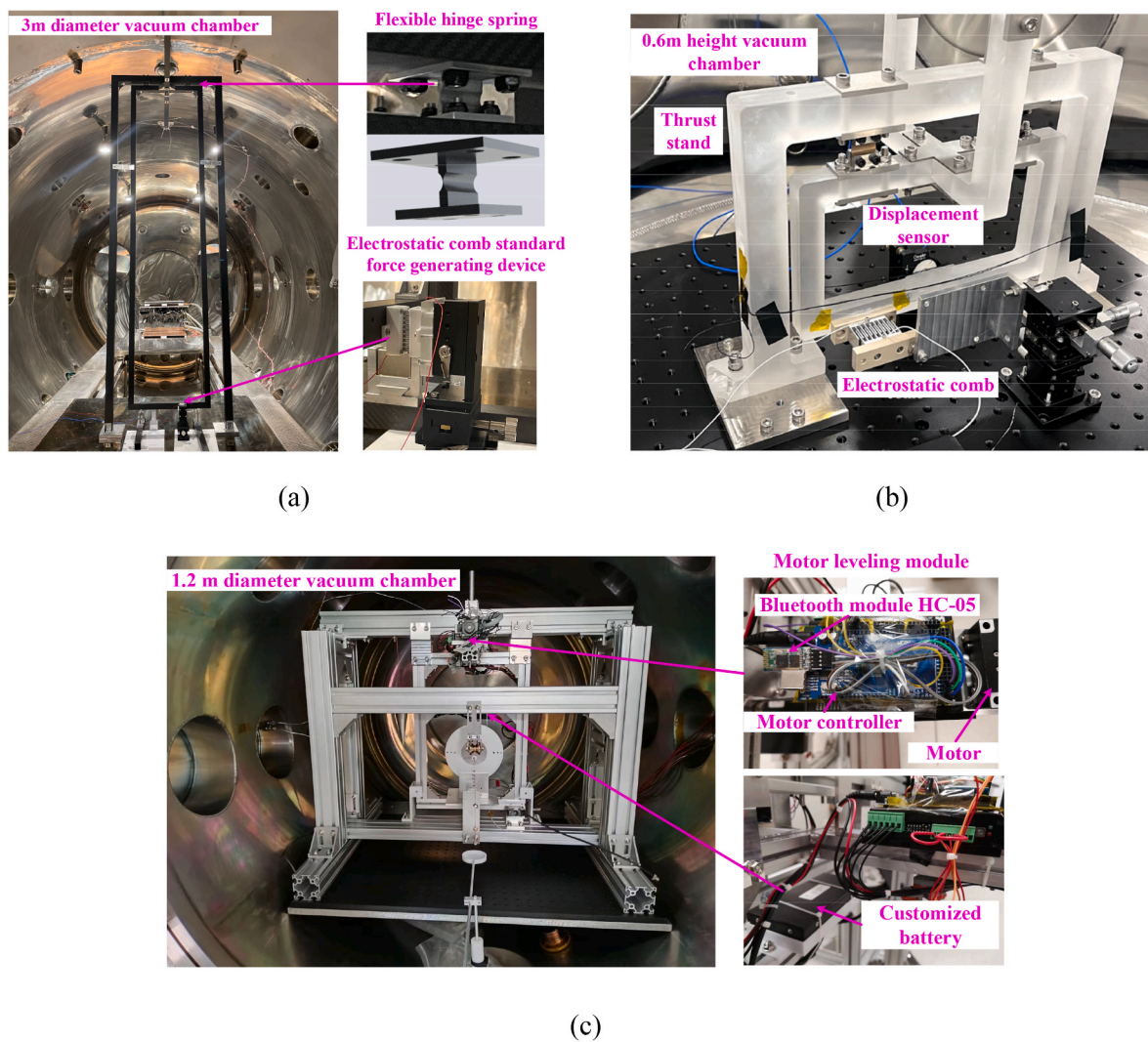


Fig. 2. The thrust stand with different topologies tested at Taiji Laboratory: (a) first generation [33]; (b) second generation [34]; and (c) third generation.

stand, the main focus of our work was to study the signal denoising algorithm.

The thrust stand's third generation, which is an iteratively updated version, is made of aluminum profiles and has a rotating arm length of 0.6 m, as shown in Fig. 2(C). To determine the horizontal state of hanging pendulums, precise leveling of the rotating arm is necessary. The first two generations of the thrust stand primarily relied on manual rough leveling by adjusting the position of the mass block on the rotating arm. However, this method has a significant margin of error and cannot be continuously adjusted during thruster operation. The third generation of the thrust stand is equipped with a stepper motor on the rotating arm for automatic leveling by adjusting the position of the mass block. An electronic accelerometer determines the tilt angle of the rotating arm. A customized battery, mounted on the arm, powers the stepper motor. All components, including the battery, stepper motor, and electrical wires, are fixed to the thrust stand as part of the rotating arm, minimizing the impact of wire sway. The Bluetooth module transmits signals to the stepper motor, allowing a researcher outside the vacuum chamber to control the motor even during thruster operation. While this design reduces the impact of wire sway and allows for remote leveling, the introduction of the motor makes it difficult to determine the system's center of gravity, and the spring may deform during motor module installation. As part of the research on the third-generation thrust stand, we conducted a preliminary investigation on the calibration of the gravity pulley method, which is widely used to calibrate milli-Newton level thrust. The test results suggest that friction at the pulley may introduce significant errors. Therefore, the electrostatic comb is a better standard force generation device for calibrating the micro-thrust stand.

The latest generation of the thrust stand was developed based on tests conducted on the previous three generations, as depicted in Fig. 3. The thrust stand is composed of an outer frame, a rotating arm, a pair of springs, a magnetic damper, a thruster mounting plate, a capacitive displacement sensor and a standard force generating device. The aluminum profiles are connected and secured by corner code connectors to form a stable outer frame. The aluminum rotating arm is connected to the crossbeam through springs and fixed to the outer frame, forming a hanging pendulum structure. The counterweight is installed at the top of the rotating arm and can be added according to actual needs.

The thruster is mounted on the thruster mounting plate, which is located on the rotating arm. Two accelerometers are used to detect the angle of the tested plane, which determines the horizontal state of the

thruster mounting plate and crossbeam. The electrostatic comb is chosen as the standard force generation device, generating weak micro-Newton force to complete the calibration of the thrust stand. The capacitive displacement sensor is mounted at the bottom of the thrust stand to measure the deflection displacement of the rotating arm. The magnetic damper consists of a copper piece and a permanent magnet, which enables the rotating arm to quickly stabilize at the final deflection state. Additionally, a displacement restrictor is installed at the bottom of the thrust stand to protect the spring and prevent unexpected deflection of the rotating arm from impacting the displacement sensor.

2.3. Thruster

Fig. 4 shows the discharge plume of the micro Hall thruster on the

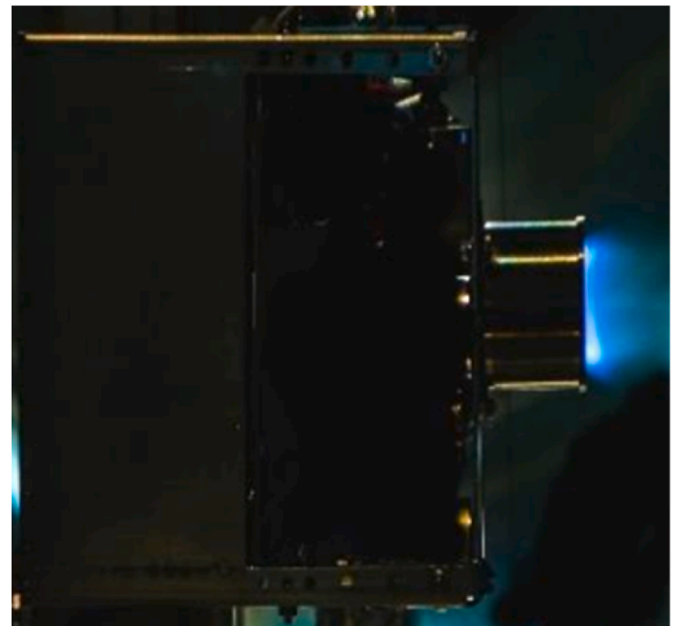


Fig. 4. The Taiji-1 satellite's micro Hall thruster plume without an external cathode [35].

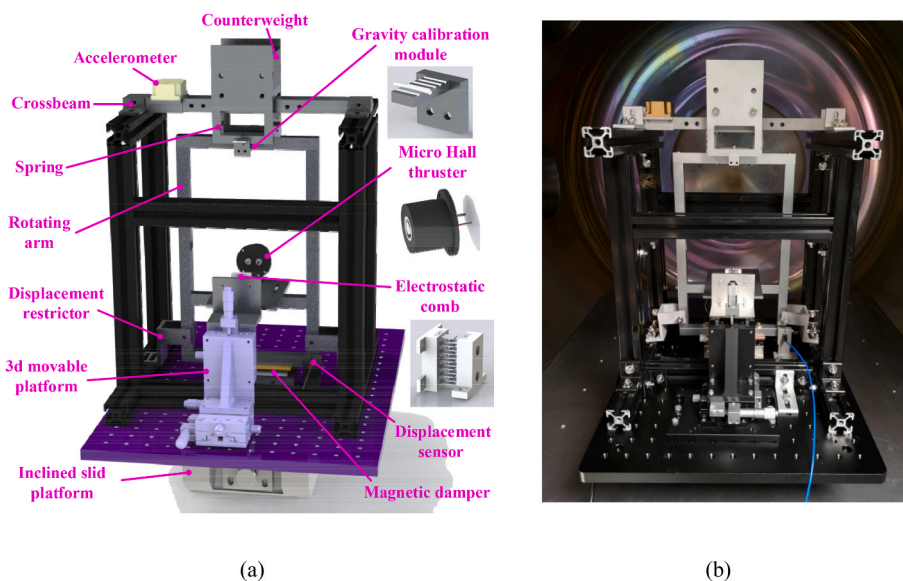


Fig. 3. The latest version of the thrust stand used for ground thrust testing of the micro Hall thruster: (a) schematic; (b) physical diagram.

Taiji-1 satellite [35]. Traditional Hall thrusters require an external cathode to initiate the plasma discharge and neutralize the plume [36, 37]. However, the micro-thrusters used in the Taiji mission must operate at extremely low power. The conventional cathode is unsuitable for this micro-thruster due to its high power consumption and big gas flow rates [38]. The thruster tested in this study is an optimized version of the Taiji-1 micro Hall thruster prototype and can operate without the need for an external cathode. Compared to the first-generation prototype from 2019, the structure and magnetic field of the thruster have been improved. Recent studies have demonstrated that micro Hall thrusters exhibit advantageous properties, such as rapid response times. In the initial phase, a probe diagnostic platform was constructed to collect electrical signals from the thruster plume region and calculate the thruster response time. The experimental findings demonstrated that under micro-Newton conditions, the thruster response time ranges from 1.08 ms to 16.76 ms [39], which can meet with the thruster response time requirements for the Taiji mission.

In the ground thrust measurement experiment of this study, the positive pole of the high-voltage power supply is directly connected to the anode of the thruster. The discharge voltage of the thruster ranges from 800 V to 2000 V. Within this anode voltage range, the temporal interval between the initiation of the high-voltage power supply and the attainment of stable voltage is measured to be less than 0.8 s. This

temporal span is shorter than the stabilization time of the thrust stand under the influence of the magnetic damper. It is imperative to acknowledge that when the thrust stand is in an oscillating state preceding stabilization, the displacement signal is excluded from the calculation. Consequently, the power supply startup time in the experiment is sufficiently brief to meet the measurement requirements. The Xe flow control system, with a resolution of 0.01 sccm, provides a xenon gas flow rate ranging from 0.1 to 0.5 sccm for the micro-thruster in the experiment.

3. Results and discussion

3.1. Thrust calibration

Before thrust measurement, it is essential to accurately calibrate the thrust stand to obtain the relationship between the deflection of the rotating arm and the force applied to it. During calibration, a standard force generating device is typically used to apply a known force to the rotating arm. The response of the rotating arm displacement can then be measured by the capacitive displacement sensor. The calibration process provides key parameters for the thrust stand, such as stiffness, resolution, and repeatability. In this study, a pair of electrostatic combs was used as the standard force generating device, which offers high accuracy

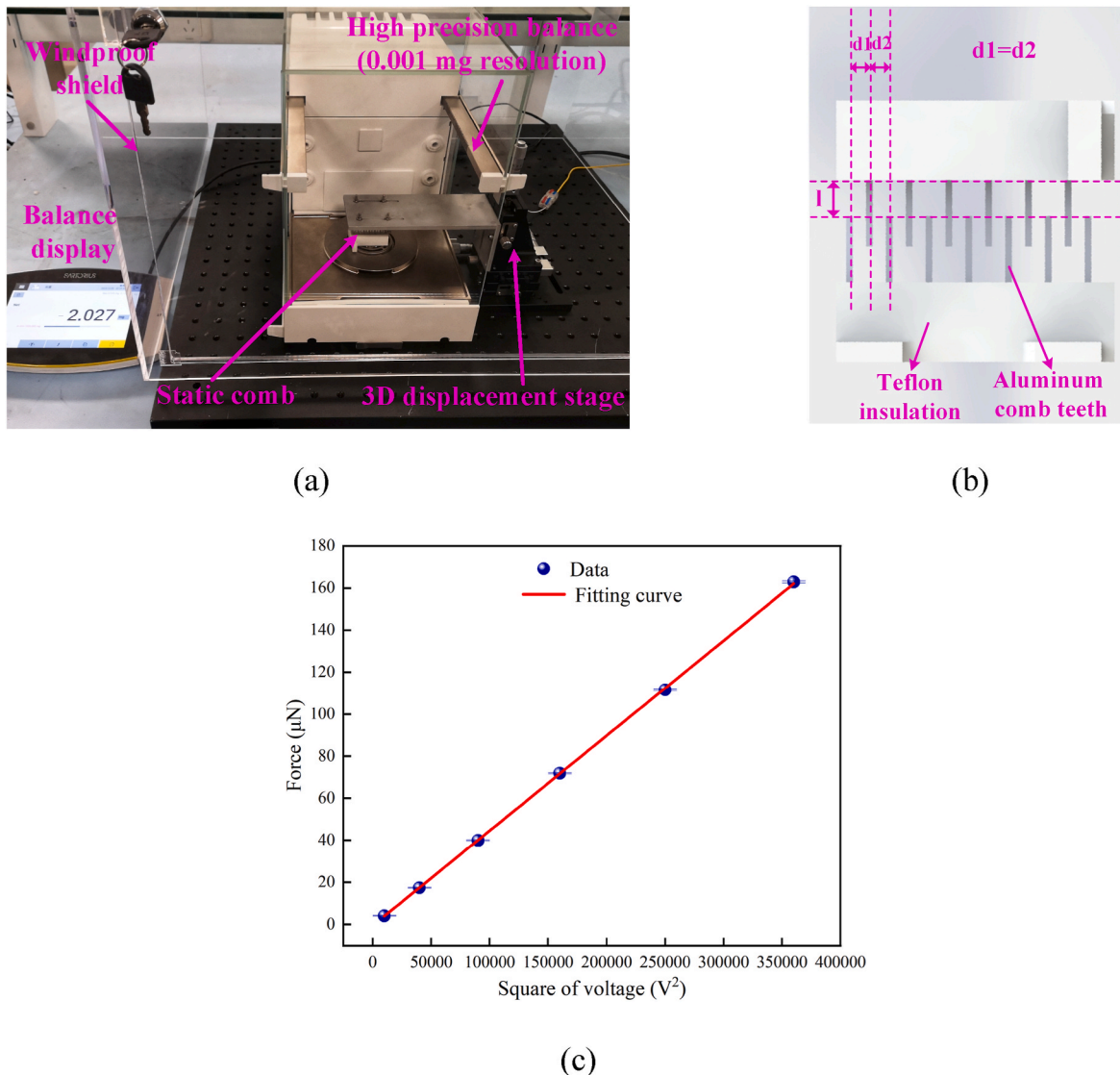


Fig. 5. Electrostatic comb test: (a) experimental platform; (b) comb teeth structure and (c) result.

and good repeatability. The weak force generated by the electrostatic comb was measured using the weighing method based on the Sartorius MCA66S-3CCN-D electronic balance. This electronic balance has a high precision with a resolution of 0.001 mg and an upper weight limit of 61 g, which can meet the accuracy and range requirements for testing. The experimental setup for the electrostatic comb test is displayed in Fig. 5 (a). The test was conducted in the second-floor underground of the Taiji laboratory, which provided a quiet environment. A windproof shield was utilized to reduce the impact of airflow on the experimental data.

A pair of electrostatic combs is comprised of two individual electrostatic combs. A single electrostatic comb is composed of aluminum comb teeth and a Teflon insulating sleeve. The two aluminum comb teeth are connected to the positive and negative electrodes of a high-voltage power supply, respectively. During the experiment, the positional relationship between the comb teeth is shown in Fig. 5(b), which is symmetrically distributed, and the electrostatic force generated is only related to the voltage.

The voltage of the electrostatic comb ranges from 0 to 600 V. Fig. 5 (c) illustrates the relationship between the force generated by the electrostatic comb and the square of the voltage, based on the electronic balance reading and the gravitational acceleration value g . The squared voltage and force are fitted using the least-square method, resulting in the relationship: $F = k \cdot V^2 + b$, where $k = 0.0004519 \mu\text{N}/\text{V}^2$, $b = 0.0024396 \mu\text{N}$, and the fitting correlation coefficient is 0.9996. The relationship between electrostatic force and voltage squared is highly linear. The results of the error bar calculations demonstrate excellent repeatability of the data, with most error bars close to zero.

The thrust measurement system's dynamic characteristics were tested using the aforementioned electric comb under different thrusts. The ground end of the electrostatic comb is mounted on the rotating arm, while the high-voltage end is installed on a three-dimensional displacement platform. According to the electronic balance test results, the known constant force is applied to the rotating arm by applying a specific voltage to the electric comb. The force is then equivalently converted to the thrust at the thruster installation position, and the corresponding deflection displacement of the rotating arm is recorded by the capacitive sensor. By varying the voltage applied to the electrostatic comb, different electrostatic forces are generated, causing the thrust at the thruster installation position to increase from 0 μN to 100 μN , as shown in Fig. 6(a). During each thrust step, the voltage on the electrostatic comb was maintained for 30 s. There is a fine linear relationship between the displacement of the rotating arm and the equivalent thrust applied to the rotating arm. The sinusoidal oscillation occurs

in the thrust stand rotating arm when the thrust changes, with the amplitude gradually decreasing due to the damping effect. After a few seconds, the oscillation stabilizes. To test the sensitivity of the thrust measurement system, a 0.1 μN pulse force was applied to analyze the system's resolution. The resulting measured thrust signal is shown in Fig. 6(b), with the red line representing the low-pass filtered result. The system demonstrates a resolution capability of better than 0.1 μN and exhibits good repeatability.

The electrostatic force generated by the electrostatic comb is selected as the standard force due to its ability to achieve a wide range and high precision. To further substantiate the precision of the electrostatic comb calibration method, gravity is used as an additional standard force to calibrate the thrust stand. The principle diagram of the gravity calibration method is shown in Fig. 7(a). The ceramic needle gauge, serving as the standard mass, is positioned within the groove of the thrust stand's gravity calibrated arm. The gravitational force of the ceramic needle gauge can be converted into the equivalent electrostatic force at the installation position of the electrostatic comb. This conversion can be achieved by measuring the distance between the ceramic needle gauge and the deflection center position, as well as the distance between the electrostatic comb and the deflection center position. By adjusting the position of the ceramic needle gauge within the groove, the relationship between the gravity-equivalent electrostatic force and the deflection displacement measured by the displacement sensor can be determined, as illustrated in Fig. 7(b). This relationship is depicted alongside the real electrostatic force generated by the electrostatic comb and the displacement. The experimental results reveals that the stiffness proportional coefficients of force and displacement demonstrate significant linear relationship and consistency under both gravity calibration and electrostatic force calibration methods. The application of the real electrostatic comb results in a linear coefficient of 19.47 between the electrostatic force and the deflection displacement, as determined by the least squares method. The R^2 value is 0.9998. The gravity calibration method yielded a linear coefficient of 19.78 between the equivalent electrostatic force and the deflection displacement, with an R^2 value of 0.9994. This observation serves to substantiate the efficacy of the electrostatic force calibration method outlined in this study.

3.2. Thruster ground thrust measurement

The micro Hall thruster's initial prototype, developed jointly by our team and Nanyang Technological University, has been launched on board the Taiji-1 satellite. The latest optimized version of the thruster

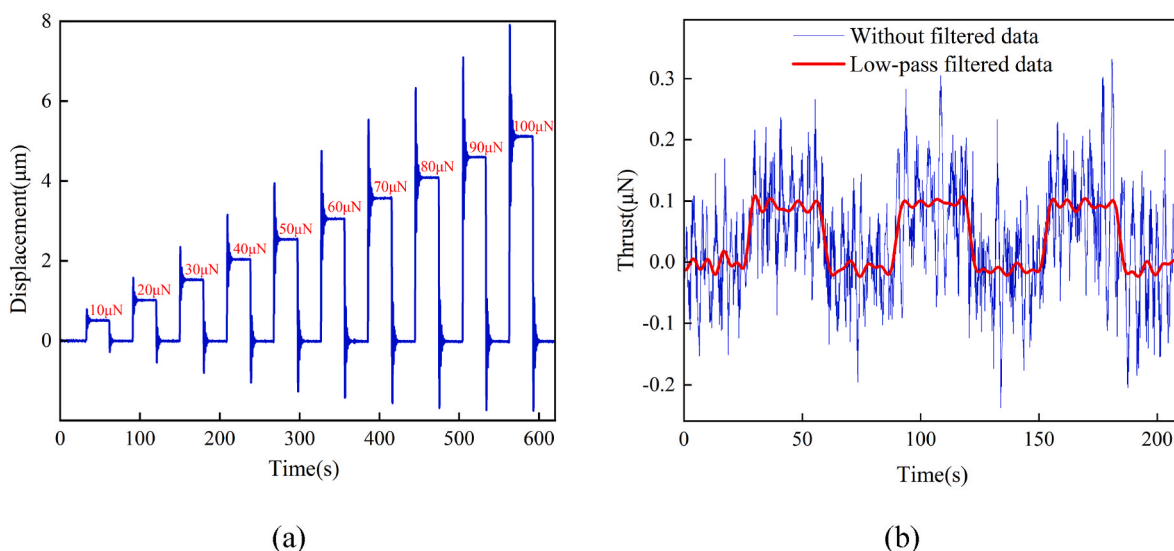


Fig. 6. (a) Response test under different thrust; (b) resolution test of the micro-thrust measurement system.

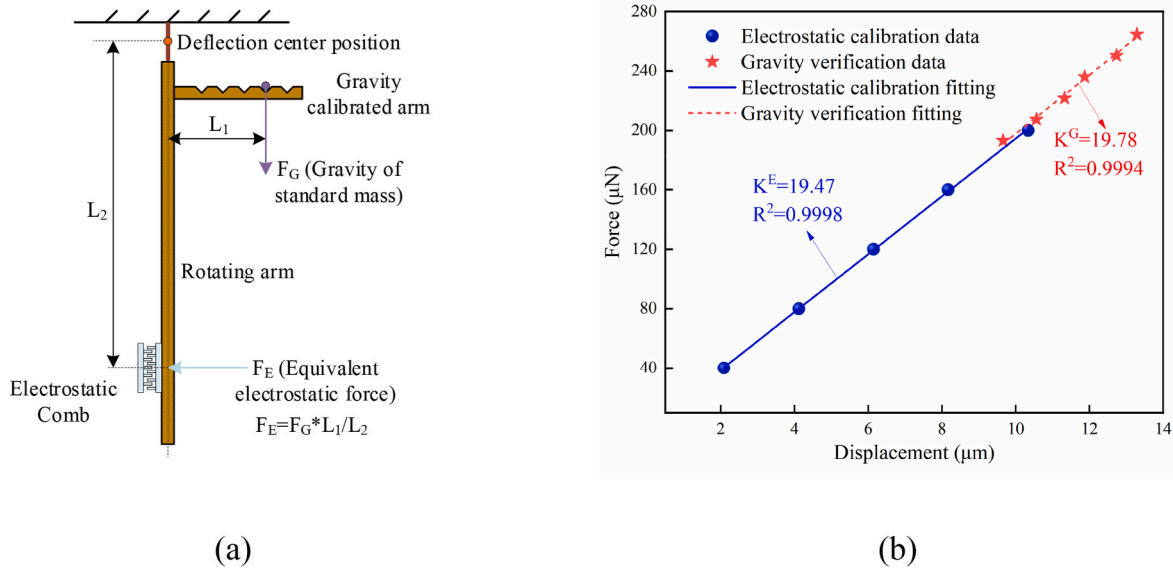
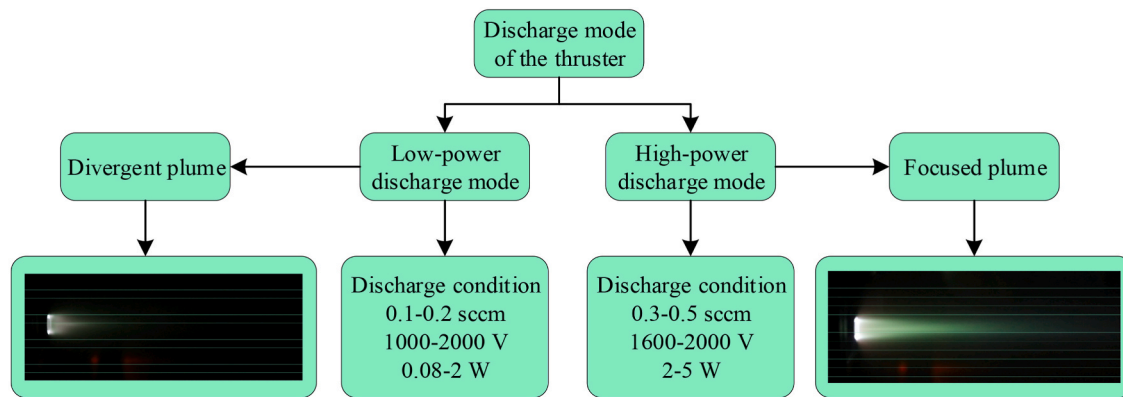


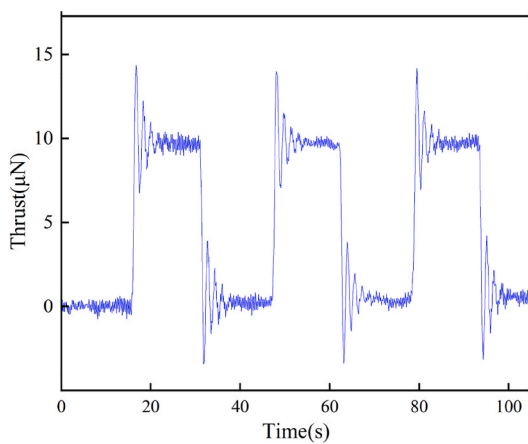
Fig. 7. (a) Gravity calibration verification method; (b) relationship between force and displacement under two calibration methods.

was tested on the thrust measurement system at the Taiji Laboratory for Gravitational Wave Universe. The thruster employs xenon as propellant, features a narrow discharge channel, and generates a magnetic field

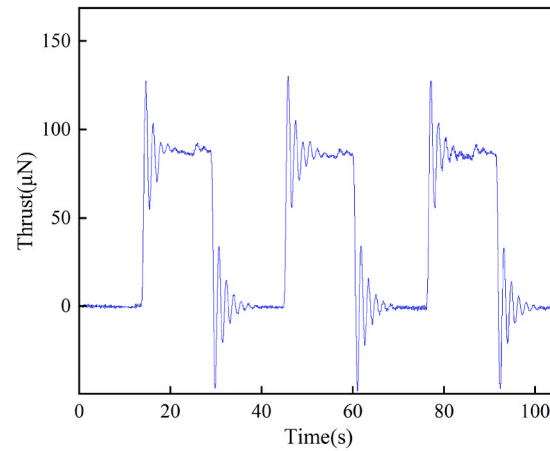
through permanent magnets. Unlike traditional Hall thrusters, this micro Hall thruster can discharge and operate without an additional external cathode. Experimental studies have shown that the thruster has



(a)



(b)



(c)

Fig. 8. (a) Thruster discharge condition; (b) switch test in low-power mode and (c) switch test in high-power mode.

two discharge modes, including the low-power mode and the high-power mode.

When the propellant flow rate of the thruster is in the range of 0.1–0.2 sccm, the thruster discharge is operating in low power mode. The discharge voltage was set at a range of 1000–2000 V, while the discharge power was recorded as 0.08–2 W. Conversely, when the propellant flow rate of the thruster is increased to 0.3 to 0.5 sccm and the discharge voltage exceeds 1600 V, the thruster discharge enters a high-power mode, with the discharge power reaching 2–5.12 W.

The plume exhibits a chaotic divergence shape under the low-power discharge mode, as shown in Fig. 8(a), while it becomes a bright convergence shape under the high-power operation mode. Dynamic response tests for the repetitive switching of the thruster were conducted under different discharge modes. The thrust signal outputs are exhibited in Fig. 8(b) and (c). The fluctuation in the thrust signal curve during thruster operation is attributed to the absence of a cathode, which leads to thruster discharge oscillation. In the subsequent work, additional physical research will be conducted to improve this problem.

The discharge voltage was adjusted to modulate the thruster's output thrust during the thruster operation as part of the thrust resolution experiment. The voltage was varied from 1000 V to 1060 V in steps of 20 V, resulting in a thrust increase from 15.78 μN to 16.27 μN . The voltage was maintained at each step for 15 s. The measured thrust variation curve is displayed in Fig. 9(a). The results show that the thrust increase is less than 0.2 μN when the discharge voltage increases by 20 V. Fig. 9(b) illustrates the range of thrust adjustment for the thruster under different discharge powers. The relationship between thrust and power follows an approximately linear trend. The increase in thrust is mainly due to the enhancement of plasma density and ion velocity inside the discharge channel. Within the power range of 0.08–5.12 W, the micro Hall thruster can continuously adjust its thrust from 0.94 to 104.67 μN .

A comparison of the thruster examined in this study with the first-generation Taiji-1 prototype reveals a significant expansion of its discharge conditions and a substantial enhancement in performance. The current version of the thruster has a higher discharge propellant flow range, from 0.1 sccm to 0.5 sccm, and the discharge voltage can reach up to 2000 V. Consequently, the thrust range has been augmented from 5 to 50 μN of the Taiji-1 prototype to the current 0.94–104.67 μN , and the thrust resolution has been elevated from 0.5 μN of the Taiji-1 prototype to 0.2 μN . The micro Hall thruster's wide thrust modulation range and simple structure make it a promising technology for future Taiji gravitational wave detection missions.

It is imperative to acknowledge the presence of inherent uncertainties in the thrust test results of the micro-Newton thruster, attributable to the confluence of systematic and random errors. According to the findings of previous research, the primary parameters that influence the micro-thrust measurement uncertainty encompass the mass value associated with the calibration force, the distance between the applied force and the deflection center, and the deflection distance as measured by the displacement sensor [40]. Of these, the mass value associated with the calibration force is contingent on the precision of the electronic balance. In order to enhance the reliability of the data, a novel 0.001 mg resolution MCA66S-3CCN-D electronic balance with a large range and high precision was utilized in this study to replace the 0.01 mg resolution electronic balance currently employed in the micro-thrust measurement field. Furthermore, experiments were conducted from 1:00 a.m. to 5:00 a.m. to mitigate environmental influences on displacement sensor readings and calibration, as this time period is characterized by minimal temperature fluctuations and environmental vibrations. Subsequent research endeavors will focus on optimizing the measurement environment of the Taiji Laboratory, with the objective of establishing a constant temperature and vibration isolation environment for the vacuum chamber. This will serve to mitigate environmental interference and reduce uncertainty in thrust measurement.

It should be noted that the vacuum chamber utilized in the ground thrust measurement experiment exhibits a relatively higher background pressure than that observed in the real space environment. The ground experiment has demonstrated that as the background pressure increases, the thrust generated by the thruster also rises as a consequence of the participation of background gas in the process of ionization. It is exceedingly challenging to achieve the same vacuum pressure in a ground vacuum chamber as in a space environment. Consequently, before the thrusters are to execute the Taiji mission, it is imperative to measure the thrust generated by the thrusters in orbit. This is done in order to correct the thrust data obtained from ground measurements, thereby ensuring that the thrusters are functioning in a normal operational mode. As demonstrated by the Taiji-1 satellite's micro Hall thruster prototype, the deployment of a gravitational reference sensor allows for the measurement of thrust while the thruster is operational in orbit, thereby facilitating accurate corrections to the ground thrust measurement data. Concurrently, the Taiji laboratory is constructing a vacuum chamber with a larger geometric scale with the objective of achieving a lower vacuum background pressure. This will provide a more realistic simulated space environment for the ground thrust measurement of the micro Hall thruster.

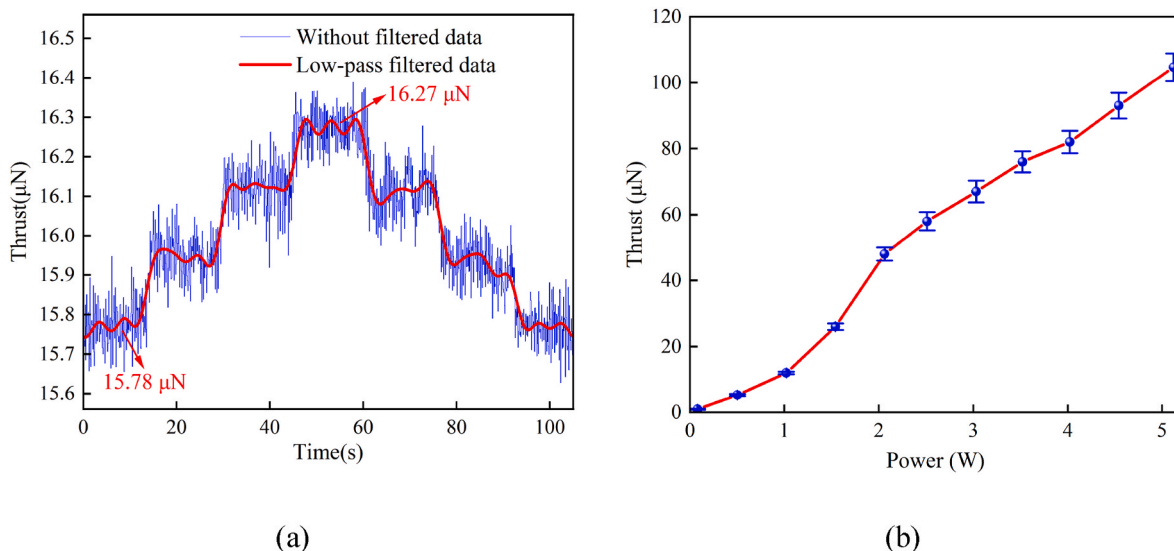


Fig. 9. (a) Thrust resolution test; (b) thrust adjustment range of the micro Hall thruster.

4. Conclusions

The Taiji Laboratory for Gravitational Wave Universe developed a thrust measurement system based on hanging pendulum technology. The thrust stand has undergone iterative optimization resulting in the latest version having a measurement range of 0–100 μN and a resolution superior to 0.1 μN . Ground thrust measurements were conducted using the optimized version of the micro Hall thruster. For this micro Hall thruster, a change of 20 V in applied voltage results in a thrust change of less than 0.2 μN . The thrust adjustment range is between 0.94 and 104.67 μN , within the power range of 0.08–5.12 W. The present study is chiefly concerned with thrust performance parameters of thrusters, and the physical processes occurring in the thruster discharge channel have not been deeply explored. In the future, it will be necessary to conduct numerical simulation of the thruster plasma discharge process to provide a theoretical basis for further optimization of the thruster. Presently, the vacuum background pressure of the ground vacuum system is still a certain distance away from the real space environment. In the future, the vacuum system will undergo optimization to reduce the extreme vacuum background pressure. Furthermore, experimental research will be carried out to explore the differences in thrust performance of thrusters in the earth and space environments.

CRedit authorship contribution statement

Shengtao Liang: Writing – review & editing, Writing – original draft, Investigation, Formal analysis, Data curation. **Luxiang Xu:** Supervision, Funding acquisition. **Shixu Lu:** Visualization, Validation, Supervision, Methodology. **Liexiao Dong:** Supervision. **Mingshan Wu:** Supervision, Conceptualization. **Jianfei Long:** Supervision.

Declaration of competing interest

The authors declare that they have no known competing financial interests or personal relationships that could have appeared to influence the work reported in this paper.

Acknowledgements

The authors would like to thank Prof. Shuyan Xu for his help in this investigation. This work is funded by the National Key R&D Program of China (2021YFC2202700), the Research Funds of Hangzhou Institute for Advanced Study, UCAS (2024HIAS-Y006), and the China Postdoctoral Science Foundation (2024M750684).

References

- [1] A. Einstein, N. Rosen, On gravitational waves, *J. Franklin Inst.* 223 (1) (1937) 43.
- [2] W. Hu, Y. Wu, The Taiji Program in Space for gravitational wave physics and the nature of gravity, *Natl. Sci. Rev.* 4 (2017) 685.
- [3] F. Antonucci, M. Armano, H. Audley, G. Auger, M. Benedetti, P. Binetruy, P. Zweifel, LISA Pathfinder: mission and status, *Classical Quant. Grav.* 28 (2011) 094001.
- [4] K. Danzmann, LISA mission overview, *Adv. Space Res.* 25 (2000) 1129.
- [5] S. Kawamura, M. Ando, N. Seto, et al., The Japanese space gravitational wave antenna: DECIGO, *Classical Quant. Grav.* 28 (2011) 094011.
- [6] Y. Gong, J. Luo, B. Wang, Concepts and status of Chinese space gravitational wave detection projects, *Nat. Astron.* 5 (2021) 881.
- [7] Z. Luo, Z. Guo, G. Jin, Y. Wu, W. Hu, A brief analysis to Taiji: Science and technology, *Results Phys.* 16 (2020) 102918.
- [8] I. Levchenko, D. Goebel, K. Bazaka, Electric propulsion of spacecraft, *Phys. Today* 75 (2022) 3.
- [9] I. Levchenko, K. Bazaka, Y. Ding, et al., Space micropropulsion systems for Cubesats and small satellites: from proximate targets to furthestmost frontiers, *Appl. Phys. Rev.* 5 (2018) 011104.
- [10] Y. Raitses, D. Staack, A. Smirnov, N.J. Fisch, Space charge saturated sheath regime and electron temperature saturation in Hall thrusters, *Phys. Plasmas* 12 (2005) 073507.
- [11] J. He, P. Liu, R. Gao, et al., Research on the neutralization control of the RF ion micropropulsion system for the ‘Taiji-1’ satellite mission, *Plasma Sci. Technol.* 22 (2020) 094002.
- [12] Y. Li, Y. Chen, S. Liu, et al., Prediction and optimization of thrust performance from plasma diagnostics in the inductively coupled plasma of an RF ion thruster, *Acta Astronaut.* 208 (2023) 130.
- [13] S. Meng, D. Yu, Effects of magnetic field configurations on the minimized ECR ion thrusters for micro-Newton and wide-range operations, *Phys. Plasmas* 30 (2023) 090702.
- [14] S. Meng, X. Zhu, D. Yu, A minimized electron cyclotron resonance ion thruster for China’s space-borne gravitational wave detection missions, *Classical Quant. Grav.* 40 (2023) 175006.
- [15] S. Yeo, H. Ogawa, D. Kahnfeld, et al., Improved modeling for design optimization of cusped field thrusters with support of kinetic analysis, *Acta Astronaut.* 195 (2022) 465.
- [16] S. Liang, H. Liu, D. Yu, Numerical simulation of magnetic field and channel configuration effect on cusped field thruster with electron cyclotron resonance discharge enhancement, *Vacuum* 204 (2022) 111376.
- [17] Z. Cai, J. Deng, Taiji scientific collaboration, satellite architecture and preliminary in-orbit experiment of taiji-1, *Int. J. Mod. Phys. A* 36 (2021) 2140020.
- [18] Taiji Scientific Collaboration, Y. Wu, Z. Luo, J. Wang, M. Bai, W. Bian, S. Yang, Taiji program in space for gravitational universe with the first run key technologies test in Taiji-1, *Int. J. Mod. Phys. A* 36 (2021) 2102002.
- [19] S. Xu, L. Xu, L. Cong, Y. Li, C. Qiao, Taiji Scientific Collaboration, First result of orbit verification of Taiji-1 hall micro thruster, *Int. J. Mod. Phys. A* 36 (2021) 2140013.
- [20] N.S. Mühlich, J. Gerger, B. Seifert, F. Aumayr, Simultaneously measured direct and indirect thrust of a FEEP thruster using novel thrust balance and beam diagnostics, *Acta Astronaut.* 197 (2022) 107.
- [21] N.S. Mühlich, J. Gerger, B. Seifert, F. Aumayr, Performance improvements of IFM Nano Thruster with highly focused ion beam generated with a compact electrostatic lens module, *Acta Astronaut.* 201 (2022) 464.
- [22] Y. Yang, S. Zhou, X. Liu, Z. Wang, W. Nie, Experimental research on micro thrust measurement of ion thruster under variable working conditions, *Vacuum* 217 (2023) 112499.
- [23] J.E. Polk, A. Pancotti, T. Haag, S. King, M. Walker, J. Blakely, J. Ziemer, Recommended practice for thrust measurement in electric propulsion testing, *J. Propul. Power* 33 (2017) 539–555.
- [24] J. Tejada, A. Knoll, A water vapour fuelled Hall Effect Thruster: characterization and comparison with oxygen, *Acta Astronaut.* 211 (2023) 702.
- [25] D. Frollani, M. Coletti, S. Gabriel, A thrust balance for low power hollow cathode thrusters, *Meas. Sci. Technol.* 25 (2014) 065902.
- [26] H. Cui, X. Li, A novel design method for the micro-thrust measurement system, *Measurement* 221 (2023) 113543.
- [27] Z. Zhang, G. Hang, J. Qi, et al., Design and fabrication of a full elastic sub-micron-Newton scale thrust measurement system for plasma micro thrusters, *Plasma Sci. Technol.* 23 (2021) 104004.
- [28] H. Xu, Y. Gao, Q. Mao, et al., A compound pendulum for thrust measurement of micro-Newton thruster, *Rev. Sci. Instrum.* 93 (2022) 064501.
- [29] L. Cong, J. Mu, Q. Liu, H. Wang, L. Wang, Y. Li, C. Qiao, Thermal noise decoupling of micro-Newton thrust measured in a torsion balance, *Symmetry* 3 (2021) 1357.
- [30] Y. Zhang, D. Guo, Y. Yang, Design and experimental validation of a micro-Newton torsional thrust balance for ionic liquid electrospray thruster, *Aerospace* 9 (2022) 545.
- [31] K. Polzin, T. Markusic, B. Stanojevic, A. DeHoyos, B. Spaun, Thrust stand for electric propulsion performance evaluation, *Rev. Sci. Instrum.* 77 (2006) 105108.
- [32] U. Kokal, E. Saridede, M. Celik, Development and tests of a thrust stand with an in-situ null position adjustment and calibration method for low power plasma thrusters, *Results Eng* 18 (2023) 101219.
- [33] X. Chen, L. Zhao, J. Xu, Z. Liu, An improved analytical model of a thrust stand with a flexure hinge structure considering stiffness drift and rotation center offset, *Actuators* 13 (2024) 21.
- [34] Z. Liu, X. Chen, J. Xu, C. Zhang, L. Xu, N. Guo, R. Yan, High-accurate robust total variation denoising algorithm with adjustable exponential upper bound function for micro-thrust measurement, *IEEE Trans. Instrum. Meas.* 72 (2023) 6504718.
- [35] G. Potrivitu, Y. Sun, M. Rohaizat, O. Cherkun, L. Xu, S. Huang, S. Xu, A review of low-power electric propulsion research at the Space Propulsion Centre Singapore, *Aerospace* 7 (2020) 67.
- [36] Y. Raitses, N.J. Fisch, Parametric investigations of a nonconventional Hall thruster, *Phys. Plasmas* 8 (2001) 2579.
- [37] Y. Raitses, A. Smirnov, N.J. Fisch, Enhanced performance of cylindrical Hall thrusters, *Appl. Phys. Lett.* 90 (2007) 221502.
- [38] D. Lee, G. Doh, H. Kim, L. Garrigues, W. Choe, Distinct discharge modes in micro Hall thruster plasmas, *Plasma Sources Sci. Technol.* 30 (2021) 035004.
- [39] L. Dong, S. Lu, N. Guo, S. Liang, J. Long, W. Luo, L. Xu, Study of the thrust response characteristics of Hall Micro Thruster, *Results Phys.* 57 (2024) 107338.
- [40] H. Zhang, B. Duan, L. Wu, Z. Hua, Z. Bao, N. Guo, Y. Ye, L. DeLuca, R. Shen, Development of a steady-state microthrust measurement stand for microspacecraft, *Measurement* 178 (2021) 109357.